RSC Advances

ROYAL SOCIETY OF CHEMISTRY

www.rsc.org/advances

Cite this: DOI: 10.1039/c0xx00000x

www.rsc.org/xxxxxx

ARTICLE TYPE

Enhancing the electrochromic response of polyaniline films by the preparation of hybrid materials based on polyaniline, chitosan and organically modified clay

Rosanny C. Silva,[a] Marina V. Sarmento,[a] Fred A.R. Nogueira,[a] Josealdo Tonholo,[a,b] Roger J. Mortimer,[b] Roselena Faez,[c] and Adriana S. Ribeiro[*,a,b]

Received (in XXX, XXX) Xth XXXXXXXXX 20XX, Accepted Xth XXXXXXXXX 20XX
DOI: 10.1039/b000000x

Polyaniline (PAni) was modified with chitosan and/or organophilic clay (Nanomer I-24) by *in situ* polymerisation using *p*-toluenesulfonic acid (PTSA) as dopant agent. These materials were characterised by FTIR spectroscopy, thermal analysis, scanning electron microscopy, d.c. electrical conductivity and spectroelectrochemical measurements. All samples maintained the electrical and electrochromic properties inherent to the PAni. Also, the addition of clay to the samples improved thermal stability and the modification of the PAni with chitosan provided the formation of homogeneous films with good adhesion onto ITO/glass electrodes as compared with pristine PAni. Using the CIE (Commission Internationale de l'Eclairage) system of colorimetry the colour stimuli of thePAni and PAni hybrid films deposited onto ITO/glass were calculated from *in situ* visible spectra recorded simultaneously to the cyclic voltammograms. Reversible changes in the hue and saturation occur in the films of all samples from yellow in the reduced state to blue in the oxidised state, but the change is much more significant for the PAni-chitosan-clay, as shown by the track of the CIE 1931 *xy* chromaticity coordinates. For the PAni-chitosan-clay film, the CIELAB 1976 colour space coordinates for a D55 illuminant were L^* = 67, a^* = -27 and b^* = 51, and L^* = 17, a^* = -22 and b^* = -5, respectively for the film in the reduced and oxidised states. These materials showed good electrochromic properties and could be applied in the assembly of electrochromic devices.

Introduction

Polyaniline (PAni), one of the most investigated conjugated polymers, finds application in the assembly of rechargeable batteries,[1] sensors,[2] and electrochromic devices.[3] It is a commercially attractive polymer because (i) it is easy to synthesise by chemical or electrochemical methods, (ii) it is environmentally stable, and (iii) its conductivity can be easily controlled by changing the doping agent. However, like other conjugated polymers, chemically synthesised PAni is difficult to obtain as a thin film, which limits its practical use.[4] Therefore, searching for chemically synthesised PAni blends and composites with better film forming properties to that of the pristine PAni is a crucial factor for their application as an electrochromic material.

In the past few years, considerable progress has been made in the preparation of PAni composites, where different materials have been incorporated with PAni in many approaches. They can be prepared by mixing PAni with other polymers in solution or in the melting state and chemically or electrochemically polymerise the monomer (aniline) in a solution containing a polymer matrix.[4] A number of polymer matrices have been used to produce conducting materials based on PAni, such as epoxy resin,[5] polyethylene,[6] poly(vinyl alcohol),[7] polystyrene,[8] poly(vinyl chloride),[9] cellulose,[10] and chitosan.[1,11,12] However, blending of PAni and non-conductive polymers usually decreases the conductivity of the composite material leading to a loss in their electrochromic response.[13,14]

Chitosan is a natural biopolymer that is usually obtained by deacetylation of chitin.[4,15] This biopolymer has the advantage of ready dissolution in dilute organic acids providing a clear, homogeneous and viscous solution,[16] which displays good mechanical properties as well as filmogenic, fibre-forming, and gelling ability, which account for an important part of its applications.[17] Furthermore, chitosan is a multifunctional polymer that can undergo easy derivatisation with specific substituents,[18] such as amines, to form a grafted copolymer as showed by Varghese and coworkers.[19]

Besides the blending of PAni and other polymers with the aim to enhance mechanical and electrochemical properties, numerous PAni composites were reported recently, including the mixture of PAni with metals, such as Ag and Au nanoparticles,[20] carbon nanotubes,[21] graphite[22] and graphene oxides,[23] and clays.[24] The main applications of these PAni composites reported in literature are for sensing, energy storage and corrosion protection,[20,21] but

just a few ones are focused in the electrochromic properties of these hybrid materials.

Clays are a good choice to prepare PAni composites aiming to enhance its electrochemical and optical properties due to the possibility of PAni intercalation inside the lamellae of the clay that can lead to a better alignment of the polymer backbone, improving its conductivity. Also layered silicate clay mineral is one of the most often investigated material because it is easily available, inexpensive, and environmentally friendly.[16]

Considering the potential application as electrochromic material of hybrids based on PAni, chitosan and an organophilic clay, we take advantage of the properties of each one to prepare a unique material bearing differentiated characteristics in a harmonised way. So in this work PAni-chitosan-clay hybrid materials were prepared and characterised. We also deposited thin films of these materials onto ITO/glass, in order to investigate their electrochromic properties and to quantify the colour changes of each hybrid material using CIE (Commission Internationale del'Eclairage) principles.[25,26]

The results obtained showed that the addition of chitosan and clay to the PAni generates materials that present harmonised properties as compared with pristine PAni, i.e. uniform films well adhered onto ITO/glass with good electrochromic response, awakening their further application in electrochromic devices assembly.

Experimental

Materials

Aniline was purchased from Synth (Brazil) and distilled before use. Ammonium persulfate ($(NH_4)_2S_2O_8$), *p*-toluenesulfonic acid (PTSA), dimethylsulfoxide (DMSO), and acetonitrile (CH_3CN) were purchased from Sigma-Aldrich; anhydrous lithium perchlorate ($LiClO_4$) was acquired from Vetec; chitosan (deacetylation degree 85 %; MW 100,000-300,000) was provided by Acros Organics. Organically modified montmorillonite clay (Nanomer I24) was supplied by Nanocor Co.

Synthesis

PAni: 0.5 mL of freshly distilled aniline was dissolved in 53 mL of 0.1 mol L^{-1} PTSA, and the solution was cooled to below -5 ^oC. A solution containing 2.14 g of $(NH_4)_2S_2O_8$ was slowly poured into the monomer solution, under vigorous stirring. The reaction temperature was maintained at -5 ^oC for 2 h. After this period, a dark green precipitate was recovered from the reaction mixture by filtration under reduced pressure and washed thoroughly with a mixture of distilled water and ethanol 10 %, until the washing liquid was completely colourless and neutral. The final product was dried under vacuum.

PAni-chitosan, PAni-clay, and PAni-chitosan-clay: PAni-chitosan samples (66.67:33.33 wt/wt) were obtained by adding 0.25 g of chitosan to 53 mL of 0.1 mol L^{-1} PTSA; the resulting solution was stirred for 2 h. Next, 0.5 mL of aniline was added to the chitosan/PTSA solution, and the mixture was stirred for 1 h.

PAni-clay samples (96.39:3.61 wt/wt) were obtained by mixing 18.8 mg of Nanomer I24 with 53 mL of 0.1 mol L^{-1} PTSA for 24 h, to swell the clay. Then, 0.5 mL of aniline was added, and stirring was maintained for 1 h.

PAni-chitosan-clay samples (65.0:32.5:2.5 wt/wt/wt) were prepared by mixing 18.8 mg of Nanomer I24 with 53 mL of 0.1 mol L^{-1} PTSA for 24 h, followed by addition of 0.25 g of chitosan and stirring for 2 h. Aniline was then added, and the solution was stirred for 1 h.

In all the preparations, the polymerisation step using $(NH_4)_2S_2O_8$ as oxidising agent was accomplished as in the case of the PAni synthesis. Table 1 shows the aniline, chitosan, and/or clay ratios used to prepare each sample.

Table 1. Proportions (in weight) of aniline, chitosan and/or clay used in the synthesis of the PAni hybrid materials.

Sample / proportions	Aniline (% wt)	Chitosan (% wt)	Clay (% wt)
PAni	100	0	0
PAni-chitosan	66.67	33.33	0
PAni-clay	96.39	0	3.61
PAni-chitosan-clay	65	32.5	2.5

Characterisation of the samples

FTIR spectra were recorded using a Shimadzu IR Prestige-21 spectrophotometer operating between 4000 and 400 cm^{-1}. X-ray diffraction (XRD) patterns of powdered samples were recorded on a Rigaku diffractometer model Miniflex using Cu-Kα radiation. Thermogravimetric analyses (TGA) were performed on a Shimadzu thermoanalyser TA-60, under nitrogen atmosphere with a flow of 100 mL min^{-1} and a heating rate of 10 ^oC min^{-1}. Differential scanning calorimetry was conducted on a Shimadzu thermoanalyser DSC-60 under N_2 atmosphere in the range 30–450 ^oC, at a heating rate of 10 ^oC min^{-1}.

Scanning electron microscopy (SEM) images of cross-sectioned pressed pellets were recorded on a JEOL field emission scanning electron microscope, model JSM 7401F using a SEI detector.

The electrical conductivity was measured by a four-point method using a Jandel Multi Height Probe with Jandel cylindrical probe head (25.4 nm diameter x 48.5 nm high), tip spacing of 1.591 nm controlled by the RM3-AR Test Unit. The pressed pellets (15 mm in diameter and 0.50 mm in thickness, respectively) used in this measurement were prepared using 120 mg of the sample. Electrical conductivity of the pressed pellet was an average of eight values measured from two sides and in different places.

Deposition of the films onto ITO/glass

100 mg of each sample (PAni, PAni-chitosan, PAni-clay and PAni-chitosan-clay) were dissolved in 1.5 mL of dimethylsulfoxide (DMSO) and maintained in an ultrasonic bath for 5 h. The films were obtained by casting 50 μL of the solutions of each sample onto ITO/glass electrodes (Delta Technologies, R_s ~10 Ω cm). The covered area of each electrode (1.0 cm^2) was delimited by an adhesive tape and the coated electrodes were allowed to dry for 48 h at room temperature in a covered container. Each film was prepared using exactly the same conditions (3.33 mg cm^{-2}) to guarantee that the films have similar thickness.

Spectroelectrochemical characterisation of the PAni hybrids films deposited onto ITO/glass

The characterisation of the films deposited onto ITO/glass electrodes was carried out using an Autolab PGSTAT30 potentiostat interfaced with a computer, using the software provided by Autolab. A one-compartment, three-electrode cell was used to characterise the films. A platinum plate was used as counter electrode and a Ag/Ag^+ (0.1 mol L^{-1} in CH_3CN) was employed as reference electrode.

The films were characterised by cyclic voltammetry in dry 0.1 mol L^{-1} $LiClO_4/CH_3CN$ solutions. Cyclic voltammograms were acquired within the fixed potential scan range of $-0.2 \leq E \leq 0.9$ V versus Ag/Ag^+ at a scan rate of 0.02 V s^{-1}. Spectra were concurrently recorded in the range 300 – 1100 nm by employing an optical glass cuvette placed in the sample compartment of a Hewlett Packard 8453 spectrophotometer.

For colour measurements a user-friendly Microsoft® Excel® spreadsheet developed by Mortimer and Varley[25,26] was used where the absorbance-wavelength data from visible region spectra were taken as input, with CIE 1931 *xy* chromaticity coordinates and luminance data generated as output. For simulation of midmorning to midafternoon natural light, the relative power distribution of a D55 constant temperature (5500 K blackbody radiation) standard illuminant was used in the calculations. Chromaticity coordinates were also transformed to *L*a*b** coordinates, a uniform colour space (CIELAB) defined by the CIE in 1976. As the chromaticity coordinates vary with film thickness[27] it is important to emphasise that all data were calculated for films prepared at the same condition, i.e. with same thickness.

Results and discussion

PAni-chitosan, PAni-clay and PAni-chitosan-clay were prepared by the emulsion polymerisation method, using ammonium persulfate as oxidant agent and PTSA as acid source. It is well known that chitosan has a good solubility in acetic acid, however PTSA was chosen to prepare the samples of the hybrid materials instead of acetic acid because PTSA is an excellent dopant agent for PAni, mainly due to its low volatility that guarantee the maintenance of the PAni conductivity for a long period of time.

Furthermore, when clay is used to prepare PAni-clay and PAni-chitosan samples it is necessary to stir the clay with the solvent for a period of 24 h before the addition of aniline or chitosan to the mixture. This procedure leads to the clay swelling and the silicate layers can be expanded and even delaminated by the organic molecules permitting the entry of the chitosan and/or aniline into their lamellae.

All samples were obtained as dark green solids, which were characterised structurally by XRD, spectroscopically by FTIR, UV-Vis, morphologically (FEG-SEM) and thermally by TG and DSC and finally by cyclic voltammetry in order to understand the influence of both chitosan and clay on electrochemical behaviour of the materials.

Structural and morphological characterization

FTIR spectra of the samples chitosan, PAni, PAni-chitosan, PAni-clay, and PAni-chitosan-clay (Figure 1a, b, c, d, and e, respectively), were recorded in order to confirm that PAni was formed and to investigate its interaction in all the systems. The peaks around 1600 (νC=C quinoid), 1500 (νC=C benzenoid), and 1300 cm^{-1} (νC-N^+.), which are typical vibrations of emeraldine salt[28] (Figure 1b) attest that PAni indeed originated during aniline polymerisation. The relative peak intensity ratios ($IC=C_{benzenoid}/IC=C_{quinoid}$) close to 1.0 indicate that PAni is in the doped state.[29] The FTIR spectrum of chitosan (Figure 1a) displays distinctive absorption bands at *c.a.* 3320 cm^{-1} ($–NH_2$ stretching) and at 1652 and 1593 cm^{-1} ($–NH_2$ bending); the band around 2870 cm^{-1} corresponds to the C–H stretching mode in chitosan,[30,31] and the absorption bands at 1151 cm^{-1} (anti-symmetric stretching of C–O–C bridge) and 1070 cm^{-1} (skeletal vibration involving the C–O stretching) are characteristic of its saccharide structure.[32,33] The bands associated with PAni remain unaltered in the FTIR spectra of the PAni-chitosan and PAni-clay systems (Figure 1c and 1d, respectively). However, the bands related to the $C=C_{benzenoid}$ and $C=C_{quinoid}$ groups are not clear in the FTIR spectrum of PAni-chitosan-clay (Figure 1e), because the chitosan bands probably override the PAni bands. To clarify the interaction between PAni and chitosan, different systems were prepared from PAni-chitosan (40/60; 50/50 and 66.7/33.3 wt. %).

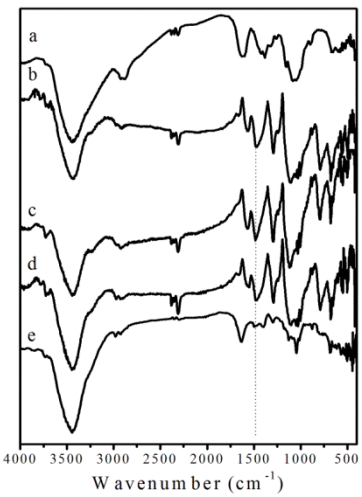

Figure 1. FTIR spectra for (a) Chitosan, (b) PAni, (c) PAni-chitosan, (d) PAni-clay, and (e) PAni-chitosan-clay.

The FTIR spectra of the PAni-chitosan samples (Figure 1–supplementary material) present the typical bands of chitosan as well as the characteristic bands of H-bonding interaction between substituted PAni and chitosan at 2908 and 3437 cm^{-1}.[33,34] These results demonstrate that a chemical linkage occurs between PAni and chitosan, suggesting the formation of a conductive copolymer as discussed in the literature.[19] Thus, if PAni and chitosan form a copolymer, we can infer that adding clay should elicit phase separation between the PAni-clay and chitosan, affording an immiscible blend. As will be discussed later, results from DSC, TG, and morphological analysis confirm this assumption.

Figure 2 depicts the XRD patterns of the clay, PAni, PAni-clay, PAni-chitosan-clay and PAni-chitosan, respectively. The XRD patterns of the composites (Figure 2c and 2d) contain a reflection at 6.7°, assigned to the d_{001} spacing of the clay (Figure 2a). The XRD pattern of PAni (Figure 2b) displays the characteristic peaks of semicrystalline PAni, and the presence of clay or chitosan does not modify this peak. For PAni-clay (Figure 2c) and PAni-chitosan-clay (Figure 2d) the XRD patterns are very similar since there is no chemical interaction between the components. However, the PAni-chitosan (Figure 2e) XRD pattern shows a decrease in the relative intensities of the peaks at 15.1° and 20.4 °, when compared to the peak at 24.6 ° related to the PAni, representing the planes (010) and (100) of the orthorhombic form of the PAni. This decrease in intensity of the peaks in PAni-chitosan can be associated to a disorder in these basal planes (010) and (100), suggesting that the formation of new chemical bonds with chitosan occurs rather in these two basal planes.[35,36] Meanwhile, the peak at 4.9° evidences increased interlayer spacing due to the presence of PAni inside the lamellae; it is less intense, though, due to the low clay content (0.05%) in the sample.

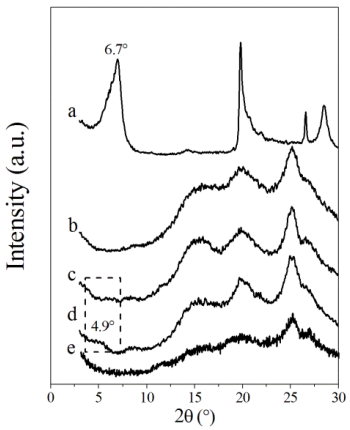

Figure 2. XRD patterns of (a) Nanomer I24 clay, (b) PAni, (c) PAni-clay, (d) PAni-chitosan-clay and (e) PAni-chitosan.

Thermal stabilities of the composites were evaluated by thermogravimetric analysis; Figure 3 presents the thermogravimetric (TG) and differential thermogravimetric (DTG) results. All the materials undergo a weight loss of *ca.* 5 % at temperatures lower than 100 °C, assigned to water loss. The doped PAni exhibits two more decomposition steps besides the water loss which are related to the release of dopant anion (~ 300 °C) and to its decomposition (280–630 °C).[37,38] For chitosan a major weight loss was found at around 300 °C which is associated to fast volatilisation of polymer segments due to thermal scission of the polymer backbone[39] corresponding to the degradation and deacetylation of chitosan.[40-42] This is similar to the results reported by other researchers.[43,44] Comparing the TG curves of the PAni hybrids (Figure 3d, e, and f) with that of pristine PAni (Figure 3b), the onset of polymer decomposition occurs at a lower temperature for the hybrids (Table 2), especially in the case of PAni-chitosan and PAni-chitosan-clay. This may be related to the influence of the volatiles from chitosan and/or PAni,[45,46] which accelerate the degradation process of the mixtures in a non-synergism effect. Comparison of theoretical curves for the hybrids, with the experimental ones confirms this effect (Figure 2-supplementary material). The simulated curves were obtained by averaging the TG curves of each pure component of the hybrid material and assuming that there were no chemical interactions between the components in the mixture during the process.[47] Furthermore, the addition of clay to the PAni-chitosan system decreases the initial degradation temperature and almost all decomposition occurs in only one stage.

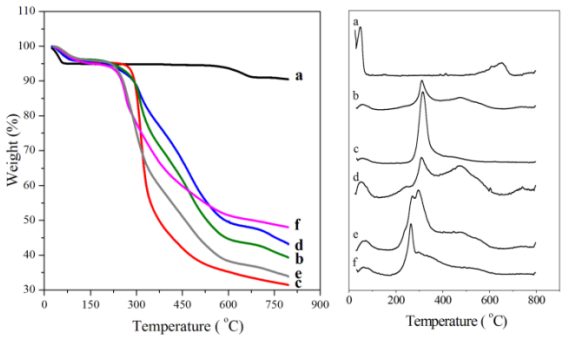

Figure 3. TG and DTG curves for (a) Nanomer I24 clay, (b) PAni, (c) Chitosan, (d) PAni-clay, (e) Pani-chitosan and (f) PAni-chitosan-clay.

In order to evaluate the glass transition temperature (T_g), the differential scanning calorimetry (DSC) curves were recorded (Figure 4). As discussed above, the PAni-chitosan does not consist only of a physical mixture between the components, as demonstrated by FTIR spectroscopy and TG analyses. The DSC results corroborate this fact: the T_g of PAni-chitosan (Figure 4c) evidences that the hybrid exhibits behaviour that is a combination of the individual behaviours of its constituents, so it can be seen as a copolymer. The T_g of the hybrid PAni-clay (Figure 4d) is lower than that of pristine PAni (Figure 4a), suggesting that the clay provides freer polymer chains; i.e., chains with greater mobility. Besides, the addition of clay in the PAni-chitosan mixture leads to the formation of two T_g values similar to their components, namely chitosan and PAni-clay.

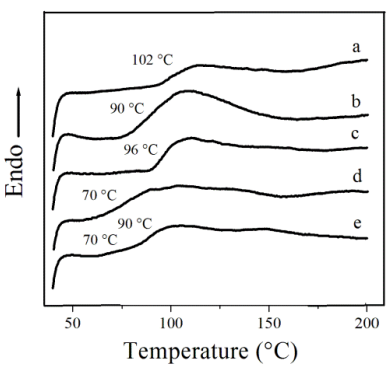

Figure 4. DSC curves of (a) PAni, (b) Chitosan, (c) PAni-chitosan, (d) PAni-clay and (e) PAni-chitosan-clay.

Table 2. Electrical Conductivity (σ), glass transition temperature (T_g), and onset temperature (T_{onset}) of chitosan, PAni, PAni-chitosan, PAni-clay, and PAni-chitosan-clay.

Materials	σ (S cm^{-1})	T_g (°C)	T_{onset} (°C)
Chitosan	-	102	286
PAni	0.50 ± 0.002	90	255
PAni-chitosan	0.56 ± 0.015	96	240
PAni-clay	0.48 ± 0.006	70	260
PAni-chitosan-clay	0.11 ± 0.026	70 and 90	233

Room temperature DC electrical conductivity values (Table 2) of PAni and its composites were measured. These materials have similar electrical conductivity, regardless of the constituents. This behaviour can be explained based on the contributions of intrachain, interchain and interparticle interactions. Since the presence of clay decreases the imperfections of the chain and particle agglomeration, the electrons can hop easily. For PAni-chitosan the formation of a copolymer generates a material with conductivity similar to the pristine PAni. According to Thanpitcha *et al.*[4] a mixture of PAni and chitosan generates a blend with low conductivity values (1.24 x 10^{-5} S cm^{-1}), whereas the copolymer PAni-chitosan obtained here affords higher conductivity (5.6 x 10^{-1} S cm^{-1}). Varghese[19] *et al.* also verified this behaviour, which agrees with the thermal and spectroscopy results, especially with the DSC data, giving further evidence that PAni-chitosan is a copolymer. Moreover, PAni-chitosan-clay also presented conductivity values of the same order of the other samples showing that the interaction between each compound is able to maintain the conductivity inherent to the PAni.

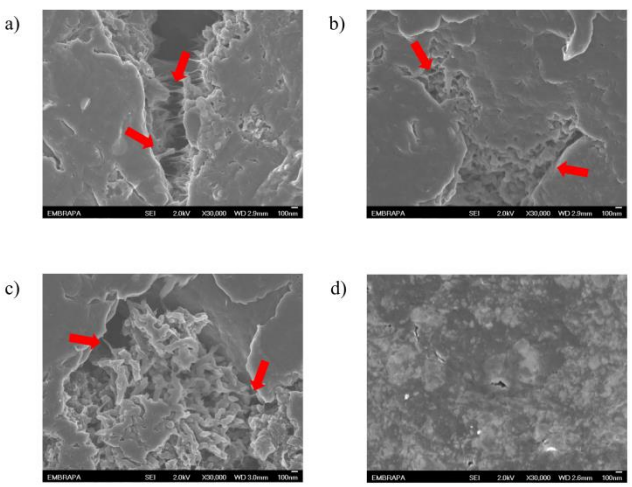

Figure 5. FEG-SEM images (x 30,000) of cross-sectioned pressed pellets of (a) PAni, (b) PAni-clay, (c) PAni-chitosan and (d) PAni-chitosan-clay.

The SEM image of PAni (Figure 5a) shows a homogeneous surface where some agglomerates are connected by fibrils. PAni-clay (Figure 5b) and PAni-chitosan (Figure 5c) SEM images show a similar morphology, even with less evident fibrils. PAni-chitosan exhibits only one phase, corroborating the DSC results; i.e., no blend arises. However, the addition of clay to PAni-chitosan mixtures disrupts the interaction between components and generates two phases (Figure 5d), which agrees with the two distinct T_g values observed by DSC.

Spectroelectrochemical characterisation

For application of these hybrid PAni films deposited onto ITO/glass as electrochromic materials, it is important to select a suitable electrolyte. Non-aqueous electrolytes offer several advantages when it comes to electrochromic devices: wider electrochemical windows and no release of hydrogen or oxygen in the operating potentials, for example. Since future electrochromic devices employing thin films of the PAni hybrid materials will be assembled using a polymer electrolyte containing $LiClO_4$, we decided to investigate the electrochemical and spectroelectrochemical properties of these films in a non-aqueous electrolyte containing $LiClO_4/CH_3CN$.

Figure 6 illustrates the cyclic voltammograms of PAni, PAni-chitosan, PAni-clay, and PAni-chitosan-clay films deposited onto ITO/glass, recorded in 1.0 mol L^{-1} $LiClO_4/CH_3CN$. Usually, PAni films in aqueous/acid medium give three peaks, around 0.2, 0.6, and higher than 0.8 V; these peaks correspond to conversion of leucoemeraldine to emeraldine, redox reactions of degradation products, and conversion of emeraldine to pernigraniline, respectively.[48] However, due to the absence of H^+ ions, the electrochemical feature of the PAni hybrid films in aprotic medium was different from the usual behaviour, showing a capacitive response and, except for PAni-chitosan-clay film, just a single defined wave.

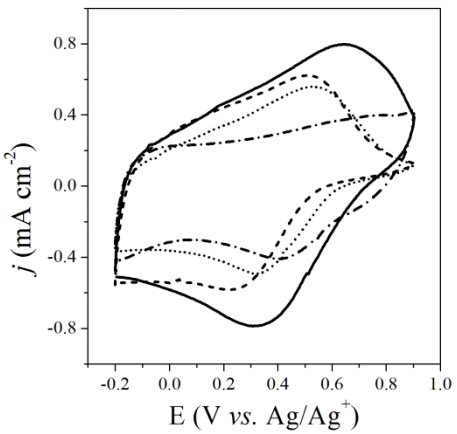

Figure 6. Cyclic voltammograms of (—) PAni, (·····) PAni-chitosan, (----) PAni-clay, and (-.-.-) PAni-chitosan-clay films deposited onto ITO/glass in 0.1 mol L^{-1} $LiClO_4/CH_3CN$, ν = 20 mV s^{-1}.

The differences between the electrochemical properties of PAni and its hybrids are clear from the comparative analysis of peak potential (Table 3). For the PAni-chitosan and PAni-clay films, the peak around 0.5 V *vs.* Ag/Ag$^+$ appears at lower anodic peak potentials as compared with pristine PAni. Concerning PAni-clay, the clay elicits freer and better oriented PAni chains, diminishing film resistance. As for PAni-chitosan, chitosan

grafting into the PAni backbone facilitates charge neutralisation upon PAni oxidation. Furthermore, copolymerisation between PAni and chitosan reduces the possibility that the protonated imine sites of PAni will undergo side reactions to generate PAni degradation products.[48]

Table 3. Anodic peak potential (E_{pa}), cathodic peak potential (E_{pc}), and λ_{max} at reduced (-0.2 V) and oxidised (0.9 V) states of the PAni, PAni-chitosan, PAni-clay, and PAni-chitosan-clay films.

Sample	E_{pa} (V)	E_{pc} (V)	λ_{max} (nm)	
			-0.2 V	0.9 V
PAni	0.64	0.31	344, 428, 870	700
PAni-chitosan	0.53	0.32	313, 433, 873	648
PAni-clay	0.51	0.22	344, 433, 870	667
PAni-chitosan-clay	0.78[a]	0.41	349, 421, 848	700[b]

[a] Badly defined peak; [b] broad band.

In situ UV–vis spectroelectrochemical studies provide information on the electronic structure of the PAni film and reveal diverse states for PAni, which depend not only on the potential, but also on the composition of the solution.[49] According to the conventional nomenclature, the main states of PAni are: (i) fully reduced leucoemeraldine, with a π–π* transition at nearly 300–350 nm and (ii) emeraldine with two absorption bands of this radical cation type species at 410–450 nm and in the NIR (> 900 nm) region. Further oxidation increases the original 1:3 ratio between quinoid and benzenoid segments in the polymer, which manifests as a blue shift in the visible range. Finally, the most oxidised form is the totally quinoid pernigraniline, which bears two positive charges on each segment (bipolaron) and absorbs at 700–800 nm.[50-52]

Figure 7 shows the UV–vis spectra of PAni and its hybrid films deposited onto ITO/glass electrodes at different potentials. All the films present the characteristic electrochromic behaviour of PAni, changing their colour from yellowish green in the reduced state to blue in the oxidised state. The spectra of PAni, PAni-chitosan, and PAni-clay films (Figure 7a, b, and c) have similar shapes; however, all the hybrid PAni films, including PAni-chitosan-clay (Figure 7d), have maximum absorption in the region 600–900 nm (oxidised state, E = 0.9 V) blue shifted by 30-52 nm when compared with the corresponding spectra of the PAni film. The band at *ca.* 430 nm appears in almost the same position in all samples; *i.e.*, it does not depend on the surrounding; hence, it must correspond to some isolated species (radical cations) localised on specific atoms (nitrogen) of PAni.[51-53] For PAni and its hybrids PAni-chitosan and PAni-clay (Figures 7a, b, and c), the absorption from the region near 800 nm shifts to the area near 650-700 nm upon increasing potential, indicating the formation of quinoid structures. In contrast, at anodic potentials, the absorption of PAni-chitosan-clay (Figure 7d) shifts to shorter wavelength less markedly. Furthermore, this band has different feature in the NIR region and is broad. Therefore, we can suggest that the formation of quinoid fragments is retarded in this case.

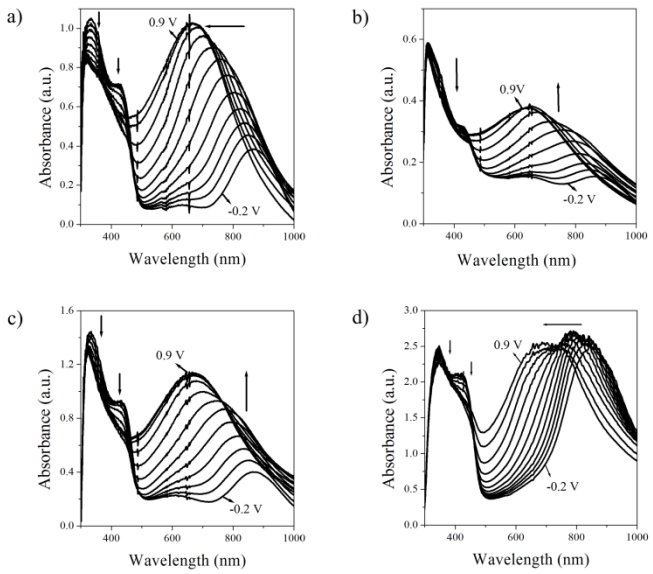

Figure 7. Absorption spectra of (a) PAni, (b) PAni-chitosan, (c) PAni-clay, and (d) PAni-chitosan-clay films deposited onto ITO/glass electrodes and measured at different potentials (from -0.2 to 0.9 V in 0.1 V intervals) in 0.1 mol L^{-1} $LiClO_4/CH_3CN$.

In colorimetry, the human eye's sensitivity to visible light is measured and a numerical description of the colour stimulus is given, thus providing a more precise way to define colour than qualitatively interpreting spectral absorption bands.[54] Figure 8 shows the CIE1931 *xy* chromaticity coordinates changes as a function of the applied potential for the PAni and PAni hybrid films as calculated from the *in situ* spectra of Figure 7. Also, the observed colours and corresponding *L*a* b** values are shown in Table 4.

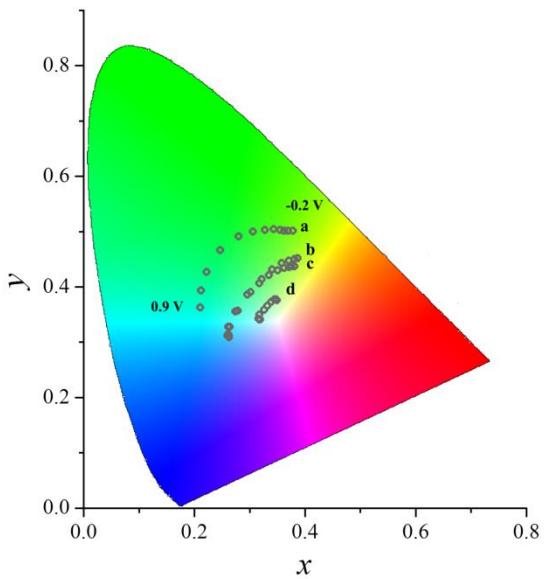

Figure 8. Calculated colour trajectory in the CIE 1931 colour space for (a) PAni-chitosan-clay, (b) PAni-clay, (c) PAni and (d) PAni-chitosan films deposited onto ITO/glass.

The CIELAB $L^*a^*b^*$ coordinates are a uniform colour space defined by CIE in 1976 and its values can be interpreted as follows: L^* is the lightness variable of the sample, while a^* and b^* correspond to the two antagonistic chromatic processes (red-green and yellow-blue, respectively). In a $L^*a^*b^*$ chromatic diagram, positive values for a^* is the red direction, negative values for a^* is the green direction, positive values for b^* is the yellow direction, and negative values for b^* is the blue direction.[54] So, in terms of CIELAB ($L^*a^*b^*$) chromaticity coordinates (Table 4), with an increase of the applied potential (from -0.2 to 0.5 V), a negative change (towards green) in a^* occurs, coupled with a dramatic negative change (towards blue) in b^*. At potentials above 0.5 V, a^* is still negative but its value become less negative while the potential increases and b^* is negative, quantifying the perceived blue colour state as a combination of green and blue at 0.9 V. This general behaviour can be observed for all samples, but the $L^*a^*b^*$ changes according to the material, being less intense for PAni-chitosan films.

Table 4. Colorimetry properties of PAni, PAni-chitosan, PAni-clay and PAni-chitosan-clay films deposited onto ITO.

Material	Potential (V)	L^*	a^*	b^*
PAni	-0.2	92	-14	42
	0.5	72	-27	4
	0.9	50	-11	-17
PAni-chitosan	-0.2	87	-4	12
	0.5	78	-6	-3
	0.9	74	-3	-5
PAni-clay	-0.2	68	-13	38
	0.5	46	-18	-4
	0.9	35	-9	-13
PAni-chitosan-clay	-0.2	67	-27	51
	0.5	46	-43	21
	0.9	17	-22	-5

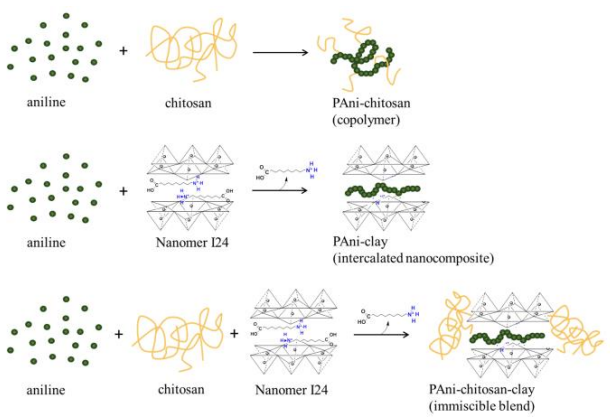

Figure 9. Schematic representation of the relationship between PAni, chitosan and clay for each hybrid material: PAni-chitosan, PAni-clay and PAni-chitosan-clay.

From the results shown in Figure 8 it is possible to observe that even though all samples change their colour from yellow at the reduced state to blue at the oxidised state this change is much more significant for the PAni-chitosan-clay. This effect agrees with the statement that the presence of chitosan and clay in the PAni structure generates a material that displays different structure and properties as compared with its individual constituents (PAni, chitosan, and clay) or its constituents combined in pairs (PAni-clay, PAni-chitosan), as shown in Figure 9.

Conclusions

The samples based on PAni, chitosan and clay were successfully prepared by *in situ* polymerisation. For PAni-chitosan a chemical linkage occurs between PAni and chitosan, forming a copolymer, otherwise, the mixture of PAni, chitosan and clay leads to a phase separation between the PAni-clay and chitosan, affording an immiscible blend. These assumptions were confirmed by the DSC, TG, and morphological analysis. All materials presented similar electrical conductivity, including PAni-chitosan, and were deposited onto ITO/glass as thin films showing electrochemical and electrochromic responses.

In summary, the addition of chitosan and/or clay in the PAni structure generates different materials that presents harmonised properties as compared with pristine PAni, awakening the possibility of application for these materials, particularly PAni-chitosan-clay, in electrochromic devices assembly.

Acknowledgements

The authors thank the granting authorities CNPq, CAPES and FAPESP (2007/50742-2) for financial support and for fellowships received by RCS (CAPES) and FARN (CAPES). The authors also acknowledge GCAR (Universidade Federal de Alagoas) for XRD and DSC analysis, Braskem Co. (Brazil) for a partnership in scientific and technological development, and Embrapa Instrum. for FEG-SEM images.

References

[1] B.-L. He, B. Dong, W. Wang and H.-L. Li, *Mater. Chem. Phys.*, 2009, **114**, 371.

[2] M. Joubert, M. Bouhadid, D. Bégué, P. Iratçabal, N. Redon, J. Desbrières and S. Reynaud, *Polymer*, 2010, **51**, 1716.

[3] Z.L. Zhao, Y. Xu, T. Qiu, L. Zhi and G. Shi, *Electrochim. Acta*, 2009, **55**, 491.

[4] T. Thanpitcha, A. Sirivat, A.M. Jamieson and R. Rujiravanit, *Carbohydr. Polym.*, 2006, **64**, 560.

[5] X. Yang, T. Zhao, Y. Yu and Y. Wei, *Synth. Met.* 2004, **142**, 57.

[6] M. Chipara, D. Hui, P.V. Notingher, M.D. Chipara, K.T. Lau and J. Sankar, *Composites Part B: Eng.*, 2003, **34**, 637.

[7] A. Mirmohseni and G.G. Wallace, *Polymer*, 2003, **44**, 3523.

[8] R.K. Gupta, R.A. Singh and S.S. Dubey, *Sep. and Purif. Technol.*, 2004, **38**, 225.

[9] R.K. Gupta and R.A. Singh, *Mater. Chem. Phys.*, 2004, **86**, 279.
[10] N.D. Luong, J.T. Korhonen, A.J. Soininen, J. Ruokolainen, L.-S. Johansson and J. Seppälä, *Eur. Polym. J.*, 2013, **49**, 335.
[11] V. Janakia, B.-T. Oh, K. Shanthic, K.-J. Leeb, A.K. Ramasamy, S. Kamala-Kannan, *Synth. Met.*, 2012, **162**, 974.
[12] C.-H. Chen, Y.-F. Dai, *Carbohydr. Polym*., 2011, **84**, 840.
[13] R. Faez, W.A. Gazotti and M.-A. De Paoli, *Polymer*, 1999, **40**, 5497.
[14] J. Bhadra and D. Sarkar, *Indian J. Pure App. Phys*., 2010, **48**, 425.
[15] S. Fuentes, P.J. Retuert, A. Ubilla, J. Fernandez and G. Onzalez, *Biomacromol.*, 2000, **1**, 239.
[16] S.S. Ray and M. Bousmina, *Progr. Mater. Sci.* 2005, **50**, 962.
[17] L. Notin, C. Viton, L. David, P. Alcouffe, C. Rochas and A. Domard, *Acta Biomater.*, 2006, **2**, 387.
[18]. M.-Y. Yin, G.L. Yuan, Y.-Q. Wu, M.-Y. Huang and Y.-Y. Jiang, *J. Mol. Catal. A: Chem.*, 1999, **147**, 93.
[19] J.G. Varghese, A.A. Kittu, P.S. Rachipudi and M.Y. Kariduraganavar, *J. Membr. Sci.*, 2010, **364**, 111.
[20] G. Ciric-Marjanovic, *Synth. Met.*, 2013, **170**, 31.
[21] P. Gajendran and R. Saraswathi, *Pure Appl. Chem.*, 2008, **80**, 2377.
[22] H. Wei, J. Zhu, S. Wu, S. Wei and Z. Guo, *Polymer*, 2013, **54**, 1820.
[23] V.H. Nguyen, L. Tang and J.-J. Shim, *Colloid Polym. Sci.*, 2013, **291**, 2237.
[24] A.F. Baldissera, J.F. Souza and C.A. Ferreira, *Synthetic Metals*, 2013, **183**, 69.
[25] R.J. Mortimer and T.S. Varley, *Displays*, 2011, **32**, 35.
[26] R.J. Mortimer and T.S. Varley, *Sol. Energy Mater. Sol. Cells*, 2012, **99**, 213.
[27] R.J. Mortimer, K.R. Graham, C.R.G. Grenier and J.R. Reynolds, *ACS Appl. Mater. Interfaces*, 2009, **1**, 2269.
[28] M. Trchová and J. Stejskal, *Pure Appl. Chem.*, 2011, **83**, 1803.
[29] N. Li, X. Li, W. Geng, T. Zhang, Y. Zuo and S. Qiu, *J. Appl. Polym. Sci.*, 2004, **93**, 1597.
[30] Y.A. Ismail, S.R. Shin, K.M. Shin, S.G. Yoon, K. Shon, S.I. Kim and S.J. Kim, *Sensor. Actuat. B: Chem.*, 2008, **129**, 834.
[31] A.G. Yavuz, A. Uygun and V.R. Bhethanabotla, *Carbohydr. Polym.*, 2009, **75**, 448.
[32] X.H. Xu, G.L. Ren, G.J. Chen, Q. Liu, D.G. Li and Q. Chen, *J. Mater. Sci.*, 2006, **41**, 4974.
[33] A.G. Yavuz, A. Uygun and V.R. Bhethanabotla, *Carbohydr. Polym.*, 2010, **81**, 712.
[34] R. Khan and M. Dhayal, *Biosens. Bioelectrochem.*, 2009, **24**, 1700-1705.
[35] J.P. Pouget, M.E. Jozefowicz , A.J. Epstein , X. Tang and A.G. MacDiarmid, *Macromol.*, 1991, **24**, 779.
[36] M. Zilberman, G.I. Titelman, A. Siegmann, Y. Haba, M. Narkis and D. Alperstein, *J. Appl. Polym. Sci.*, 1997, 66, 243.
[37] M.V. Kulkarni and A.K. Viswanath, *J. Macromol. Sci., Part A*, 2004, **41**, 1173.
[38] P. Gajendran and R. Saraswathi, *Pure Appl. Chem.*, 2008, **80**, 2377.
[39] A. Khan, R.A. Khan, S. Salmieri, C.L. Tien, B. Riedl, J. Bouchard, G. Chauve, V. Tan, M.R. Kamal and M. Lacroix, *Carbohydr. Polym.*, 2012, **90**, 1601.
[40] S.F. Wang,, L. Shen, Y.J. Tong, L. Chen, I.Y. Phang, P.Q. Lim and T.X Liu, *Polym. Degrad. Stab.*, 2005, **90**, 123.
[41] X. Wang, Y. Du, J. Yang, X. Wang, X. Shi and Y. Hu, *Polymer*, 2006, **47**, 6738.
[42] M. Lavorgna, F. Piscitelli, P. Mangiacapra and G.G. Buonocore, *Carbohydr. Polym.*, 2010, **82**, 291.
[43] F.A.A. Tirkistani, *Polym. Degrad. Stab.*, 1998, **60**, 67.
[44] X. Qu, A. Wirsen and A.C. Albertsson, *Polymer*, 2000, **41**, 4841.
[45] L. Zeng, C. Qin, L. Wang and W. Li, *Carbohydr. Polym.* 2011, **83**, 1553
[46] M.K. Traore, W.T.K. Stevenson, B.J. McCormick, R.C. Dorey, S. Wen and D. Meyers, *Synth. Met.*, 1991, **40**, 137.
[47] W.A. Gazotti Jr., R. Faez and M.-A. De Paoli, *Eur. Polym. J.*, 1999, **35**, 35.
[48] L.-M. Huang, C.-H. Chen, T.-C. Wen and A. Gopalan, *Electrochim. Acta*, 2006, **51**, 2756.
[49] P.S. Tóth, G.S. Samu, B. Endrödi and C. Visy, *Electrochim. Acta*, 2013, **110,** 446.
[50] A.H.A. Shah and R. Holze, *Synth. Met.*, 2006, **156**, 566.
[51] A.A. Nekrasov, O.L. Gribkova, T.V. Eremina, A.A. Isakova, V.F Ivanov, V.A. Tverskoj and A.V. Vannikov, *Electrochim. Acta*, 2008, **53**, 3789.
[52] F.F.C. Bazito, L.T. Silveira, R.M. Torresi and S.I.C. Torresi, *Phys. Chem. Chem. Phys.*, 2008, **10**, 1457.
[53] S. Pahal, M. Deepa, S. Bhandari, K.N. Sood and A.K. Srivastava, *Sol. Energy Mater. Sol. Cells*, 2010, **94**, 1064.
[54] G. Wyszecki, W.S. Stiles, Color Science: Concepts and Methods, Quantitative Data and Formulae, 2nd ed., John Wiley and Sons, New York, 1982.

[a] *Instituto de Química e Biotecnologia, Universidade Federal de Alagoas, Campus A.C. Simões, Tabuleiro do Martins, 57072-970, Maceió-AL, Brazil.*
[b] *Department of Chemistry, Loughborough University, Loughborough, Leicestershire, LE11 3TU, United Kingdom.*
[c] *Laboratório de Materiais Poliméricos e Biossorventes, Universidade Federal de São Carlos, Campus Araras, Araras-SP, Brazil.*
* *Corresponding author: Adriana S. Ribeiro; E-mail: aribeiro@qui.ufal.br.*
†Electronic Supplementary Information (ESI) available: [details of any supplementary information available should be included here]. See DOI: 10.1039/b000000x/

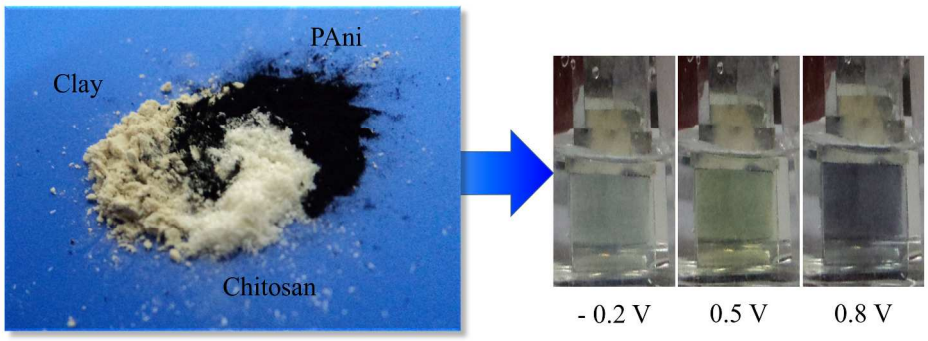

800x400mm (96 x 96 DPI)

Highlights

Electrochromic materials based on PAni, chitosan and clay show distinct colour variation depending on the compound present in the hybrid material.